PRS/RPT-23-03913
Revision 0

Development Plan for Acoustic Emission and Vibration Sensors

November 2023

Joshua Daw
Bibo Zhong

Idaho National Laboratory

INL is a U.S. Department of Energy National Laboratory operated by Batelle Energy Alliance, LLC

PRS/RPT-23-03913
Revision 0

Development Plan for Acoustic Emission and Vibration Sensors

Joshua Daw
Bibo Zhong

November 2023

Idaho National Laboratory
Measurement Sciences Laboratory
Idaho Falls, Idaho 83415

http://www.inl.gov

Prepared for the
U.S. Department of Energy
Office of Nuclear Energy
Under DOE Idaho Operations Office
Contract DE-AC07-05ID14517

Page intentionally left blank

SUMMARY

This document discusses the need for high-temperature, radiation-tolerant sensors to monitor vibrations and acoustic emissions (AEs) in advanced reactors and irradiation experiments. Several commercial sensors were tested using infrastructure available at Idaho National Laboratory to benchmark both the currently available sensors as well as the test facilities, leading to a development strategy for sensors capable of withstanding more extreme environments.

Page intentionally left blank

CONTENTS

FIGURES

TABLES

ACRONYMS

AE	acoustic emission
EMI	electromagnetic interference
FAS	flowing autoclave system
FFT	fast Fourier transform
LDV	laser doppler vibrometer
PLB	pencil lead break
TREAT	Transient Reactor Test Facility

Page intentionally left blank

1. INTRODUCTION

The advanced reactor types currently under development generally operate at higher temperatures than light-water reactors and utilize coolants that may be highly corrosive (i.e., liquid metals). The combination of an elevated temperature and a more extreme chemical environment will exacerbate aging mechanisms such as high-temperature creep and fatigue. Monitoring such mechanisms and detecting damage prior to failure requires nondestructive evaluation/testing and/or structural health monitoring techniques. [1] Though many technologies are available for structural health monitoring, ultrasonic and acoustic methods are of particular interest given their current widespread use in other industries, their flexibility in terms of operating conditions, and their ability to detect damage either passively or actively—as well as internally to a material or part. Acoustic emission (AE) signals represent acoustic energy released within a material as a result of microstructural damage. Figure 1 shows a typical AE signal, with all the features of interest labeled.

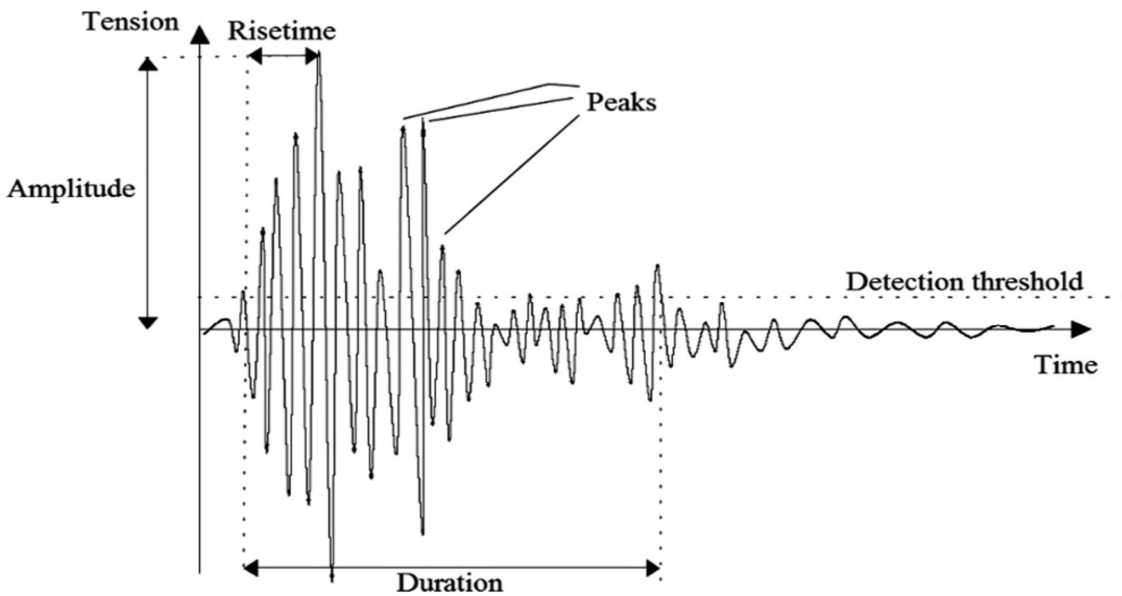

Figure 1. General features of an AE signal. [1]

The amplitude is the maximum voltage detected in a waveform. To detect AE signals, a voltage threshold is used to discriminate noise signals from real AE signals. The rise time represents the period between the first threshold crossing and the peak voltage. Rise time is related to the wave propagation between the source of the AE event and the sensor. Duration is the length of time between the first and last threshold crossings, and is related to the total energy of the AE signal. The number of peaks between the first and last threshold crossing are related to the counts is the area under the rectified curve. and gives an estimate of the total energy of the AE event.

Low-frequency-range (10–100 kHz) emissions can be associated with macroscopic events such as pellet-cladding interactions, fuel-cladding mechanical interactions, and fuel rod vibrations. These low-frequency events can be indicative of structural changes, fuel swelling, or mechanical interactions within the fuel assembly. This frequency range also includes phenomena such as boiling and leakage in sodium fast reactors, in which signals have been observed with frequency content up to 10 kHz. [2-3]

Medium-frequency-range (100 kHz to 1 MHz) AEs are often encountered in nuclear fuel and cladding studies. These emissions can originate from microstructural changes (e.g., crack initiation and propagation [4]) in the fuel pellets or cladding material. Medium-frequency events are particularly relevant when investigating fuel performance, cladding integrity, and failure mechanisms.

High-frequency-range (1 MHz and above) AEs can occur in nuclear fuel and cladding systems, due to phenomena such as rapid crack growth, microfracture propagation, or interactions with high-energy particles (e.g., fission products). High-frequency events may be of interest when assessing the structural integrity and behavior of fuel rods and cladding under extreme conditions.

Not all low-frequency-range phenomena should be classified as AEs. In an AE event, released energy travels through the material as microscopic strain. In other cases such as flow-induced vibration (typically in the low kHz range [5]), the energy transmission is macroscopic in nature and results in bulk motion of the part under consideration. In these cases, a different sensor known as an accelerometer is used for taking measurements. The difference between the two sensor types is that the accelerometer (or vibrometer) contains a seismic mass that is in contact with the sensing element. Including this mass enables the measurement of forces, not simply motion detection. Generally, an AE sensor detects transient signals transmitted through the bulk of a material, whereas an accelerometer allows for longer-term monitoring of the bulk motion of a system. Acoustic coupling is much more important with AE measurements than with vibration monitoring. While AE sensors passively detect active damage mechanisms (and only active mechanisms produce AE signals [6]), accelerometers can measure the overall health of dynamic systems by enabling the system state to be monitored as a function of vibrational frequencies. In other words, by monitoring all the vibratory frequencies present, damage can be detected as a change to the frequency spectrum over time. [7], [8]

2. NEED FOR ACOUSTIC EMISSION AND VIBRATION SENSORS IN NUCLEAR INDUSTRY/RESEARCH

Vibration and AE sensors are needed for a wide range of applications in the nuclear field. For power reactors, overall system condition monitoring is achievable via monitoring and analysis of the vibration state of components (e.g., pumps and flow pipes). Changes in frequencies or amplitudes generally indicate damage, flow pipe fouling, loose parts, etc. Flow-induced vibrations can also be used as a measure of flow rates. AE monitoring can be utilized to track known material defects, detect and locate leaks, or identify loose parts. In research applications, AE sensors can detect crack propagation in tensile test specimens, oxide fuel cracking, onset of boiling, and cladding failures.

3. CURRENT TECHNOLOGY ASSESSMENT

Commercial sensors are currently available from several manufacturers, [1] and those sensors based on piezoelectric materials overwhelmingly dominate the market. Piezoelectric materials are typically suitable only at low temperatures and in the absence of neutron or gamma radiation. Some materials have been identified [9] that can operate at higher temperatures (>1000℃) and survive certain levels of gamma and neutron radiation. However, these materials have yet to be adopted by commercial vendors. Newer piezoelectric materials with great potential have been postulated as possessing high radiation tolerance, but have not yet been tested in this regard. [10] Furthermore, other base technologies (e.g., magnetostrictive materials) are less developed for use than AE or vibration sensors.

A developmental vibration sensor/accelerometer based on a high-temperature, radiation-tolerant material called aluminum nitride has been under development by researchers at North Carolina State University. [11] The basic concept of their high-temperature embedded/integrated sensors system has been demonstrated, but the sensor requires much more development before being considered viable for widespread use. Furthermore, aluminum nitride is known to possess low sensitivity and may be inappropriate for AE sensors, which require high sensitivity in order to detect microscopic displacements.

To benchmark the current state of the technology, as well as the relevant Idaho National Laboratory testing infrastructure, several high-temperature-capable commercial AE sensors and accelerometers were purchased and tested. These were all advertised as being gamma-radiation-tolerant and possessing relatively low neutron fluence. The AE sensors were tested on benchtop, in furnaces, and in the Transient Reactor Test Facility (TREAT). The accelerometers were tested on benchtop and in the Measurement Sciences Laboratory's flowing autoclave facility.

3.1 AE Sensor Testing

3.1.1 Furnace Testing

Figure 2 shows the experimental setup for testing the high-temperature performance of AE sensors. An AE sensor was clamped onto a steel bar that was 1/8 in. thick, 1 in. wide, and 30 in. long. Aluminum foil was used to couple the AE sensor to the steel bar. Subsequently, both the sensor and the bar were placed inside a high-temperature furnace.

The AE sensor's performance was evaluated at increasing temperatures via a pencil-lead break (PLB) test, in which a piece of pencil lead (typically 0.5 or 0.3 mm in diameter) is broken approximately 3 mm from its tip by pressing it against the surface of the object being tested. [1] This process generates a powerful acoustic signal that closely resembles a natural AE source. The sensors detect this signal as a strong burst. Signals obtained from PLBs are highly consistent, provided the mechanical pencil is handled in exactly the same manner each time.

For each temperature level, the AE system's peak voltage output was noted. To obtain an average, three PLB tests were conducted.

Figure 2. Experimental setup for testing the high-temperature performance of the AE sensor.

Table 1. PLB results for the AE sensor at increasing temperatures.

Temperature (°C)	1st PLB (mV)	2nd PLB (mV)	3rd PLB (mV)	Average (mV)
22	800	650	800	750
100	600	800	800	733
200	800	1000	600	800
300	600	600	1000	733
400	600	600	800	667
500	700	800	600	700
600	N/A	N/A	N/A	N/A

Table 1 displays the results of the PLB tests conducted at various temperature levels. The AE sensor functioned effectively at up to 500°C, without any sign of degradation. However, at 600°C, the sensor failed to respond, indicating it had ceased to function. Even after cooling the furnace back down to room temperature, the AE sensor failed to produce any signals, confirming it was no longer operational.

The PLB test results validated the operational high-temperature range specified by the manufacturer. Specifically, the commercial AE sensor was found to function effectively at up to approximately 540°C.

3.1.2 TREAT Testing

3.1.2.1 Experiment THOR MOXTOP 1

The TREAT experiment referred to as THOR MOXTOP 1t utilized two AE sensors. The sensor for channel 1 was affixed within the test capsule; the sensor for channel 2 was employed to detect the trigger from TREAT for time stamping, as the commercial AE system does not have an external trigger.

The times of the events detected by channels 1 and 2 were recorded and the corresponding waveforms extracted. From channel 2 (trigger channel), two events were recorded, reflecting the start and end of the reactor transient. The total transient time from channel 2 on the AE system was 18 seconds. After determining the start and end of the reactor transient, the events detected by channel 1 during the transient were then extracted.

In total, eight events were recorded during the 18-second transient. (See Table 2 for their times of occurrence.) Figure 3 shows the captured event from channel 1 at 9.0772 seconds after the transient trigger signal, and all of the other waveforms look similar to this waveform.

Table 2. Times of the events detected by channel 1, relative to the trigger.

Event #	**1**	**2**	**3**	**4**	**5**	**6**	**7**	**8**
Time after trigger (s)	9.077	9.676	9.729	10.169	10.416	10.510	11.519	11.529

Two characteristics of the waveforms were extracted: maximum amplitudes and the frequencies with the highest energy, as shown in Figure 4 and Figure Figure 5, respectively.

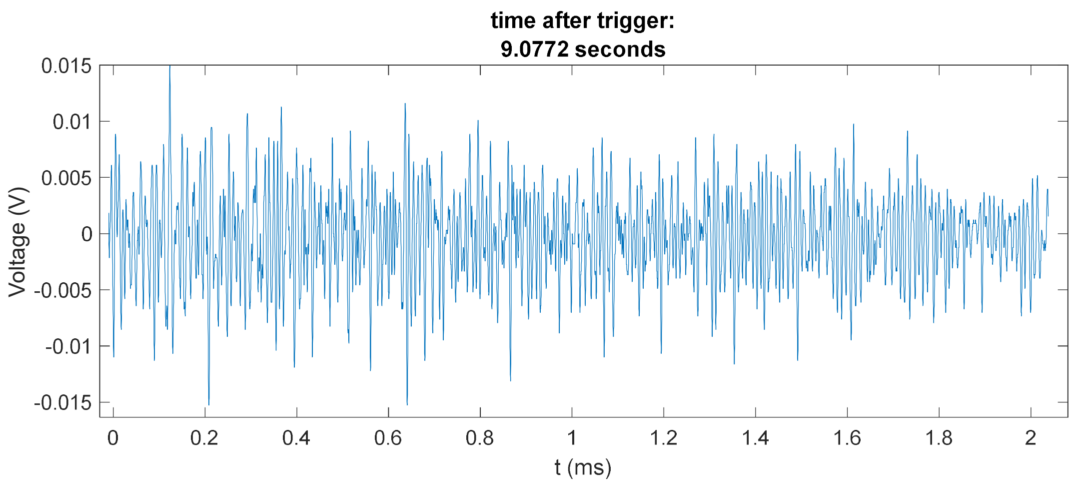

Figure 3. Waveform detected by channel 1 at 9.0772 seconds after the trigger.

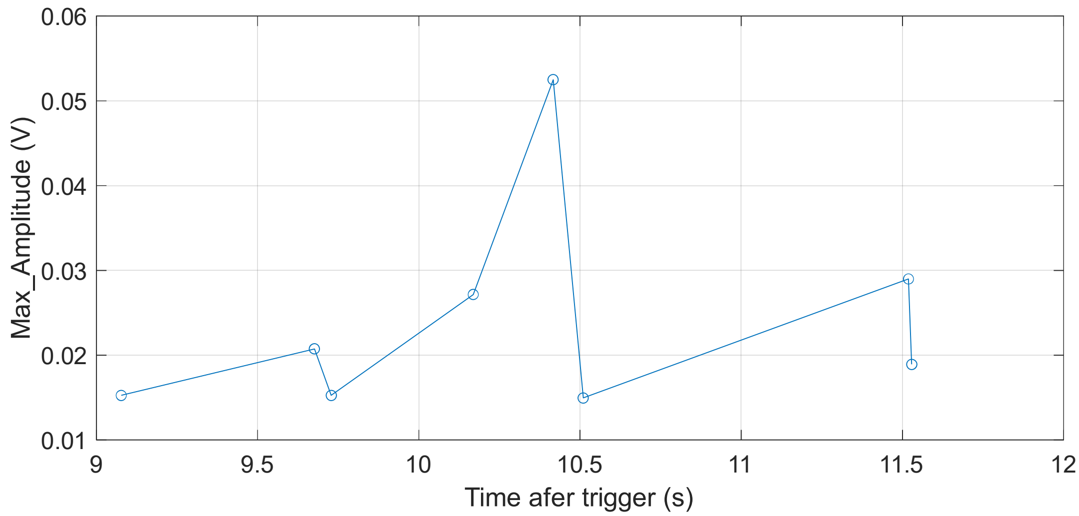

Figure 4. Maximum amplitudes of the waveforms captured by channel 1.

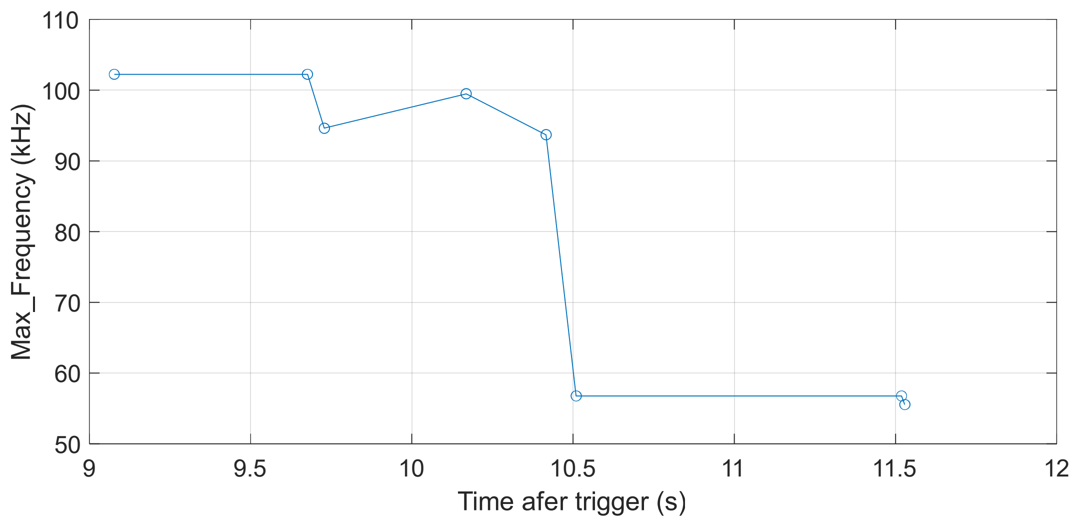

Figure 5. Highest-energy frequencies of the waveforms captured by channel 1.

3.1.2.2 Experiment LOC C1

The experimental setup in the LOC C1 test was identical to that in THOR MOXTOP 1. In this test, the total time of the transient was 30 seconds. A total of 21 events were detected by channel 1. (See Table 3 for the times of occurrence.) Similarly, the maximum amplitudes and the frequencies with the highest energy are presented in Figure 6 and Figure Figure 7.

Table 3. Timing of the events detected by channel 1, relative to the trigger.

Event #	**1**	**2**	**3**	**4**	**5**	**6**	**7**	**8**	**9**	**10**	**11**
Time after trigger (s)	2.873	2.916	2.983	2.999	3.031	3.045	3.064	3.087	3.094	3.106	3.108
Event #	**12**	**13**	**14**	**15**	**16**	**17**	**18**	**19**	**20**	**21**	
Time after trigger (s)	3.119	3.128	3.148	3.153	3.182	3.191	3.221	3.390	3.393	3.493	

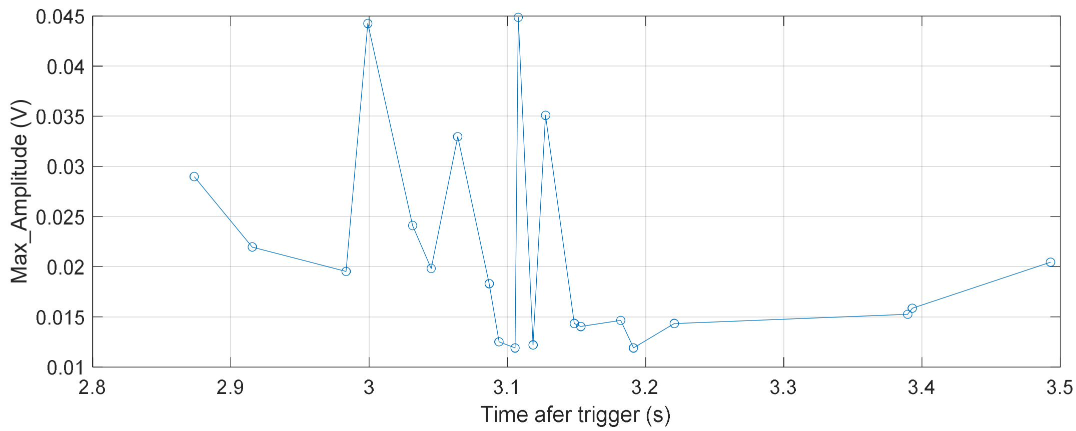

Figure 6. Maximum amplitudes of the waveforms captured by channel 1.

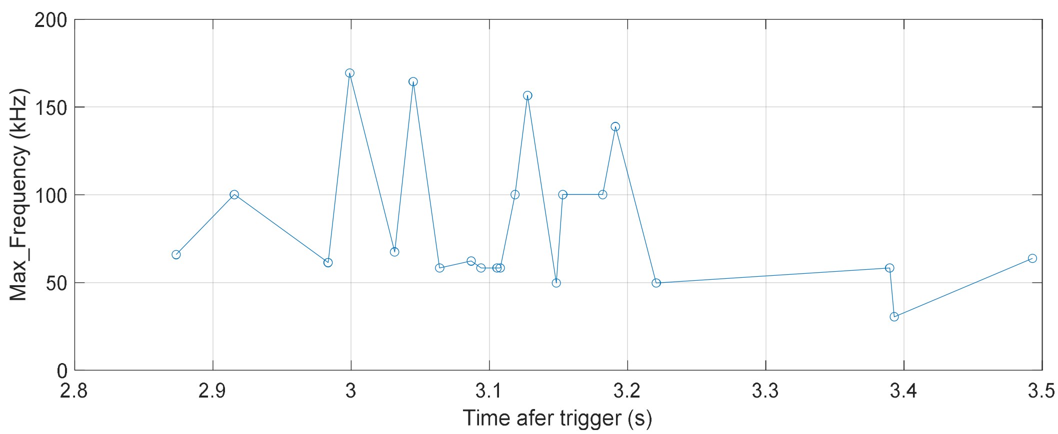

Figure 7. Highest-energy frequencies of the waveforms captured by channel 1.

To date, all AE sensors tested in TREAT have survived the irradiations. This is important despite the relatively low power of these irradiations.

3.2 ACCELEROMETER TESTING

The next two experiments experiment evaluated the performance of a commercial accelerometer and a laser doppler vibrometer (LDV) at measuring vibrations in the main pipe of the Measurement Sciences Laboratory's flowing autoclave system (FAS), the goal being to benchmark both the sensor performance and the FAS as a test facility.

Vibrations in the stainless-steel main pipe of the FAS were measured by clamping the accelerometer to the center of the pipe. The LDV's measurement point was directly above the accelerometer, and a small piece of light diffuser film ensured that the light received was of a sufficiently high intensity. Figure 8 illustrates the experimental setup and measurement locations. The accelerometer and LDV outputs were both simultaneously digitized using a USB oscilloscope featuring a set sampling rate of 20 kHz.

Two separate experiments were conducted. The first involved measuring vibrations at varying water pump frequencies of 10–75 Hz, using increments of 10 Hz. Each individual measurement lasted 20 seconds. The second experiment entailed continuous vibration measurement while altering the water pump frequency from 65 to 75 to 5 Hz, before finally turning the pump off completely. This experiment lasted a total of 500 seconds.

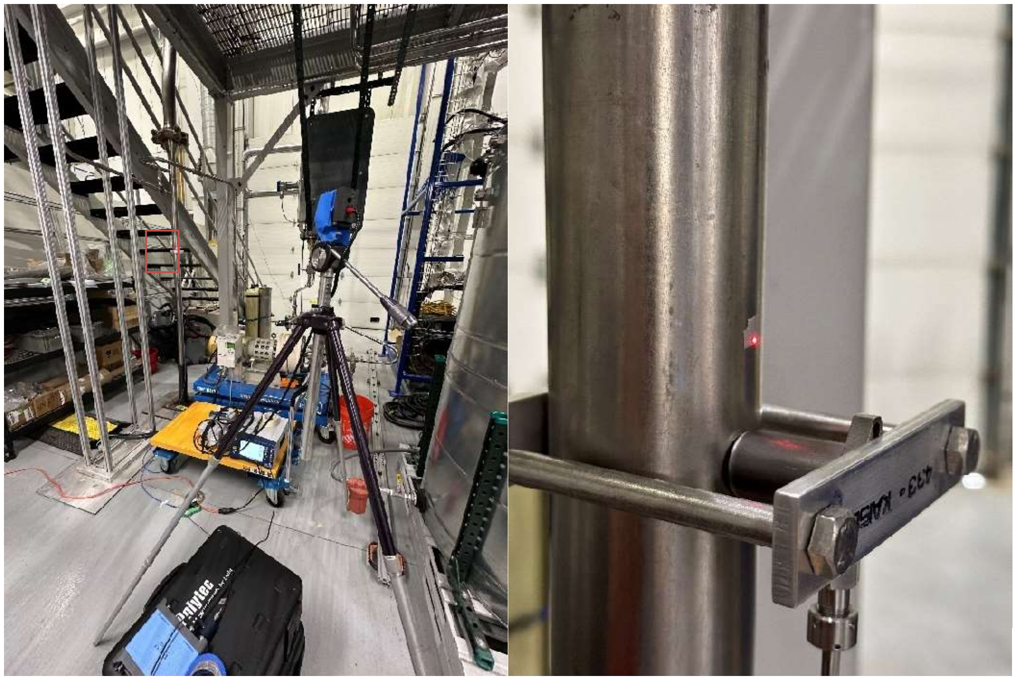

Figure 8. Experimental setup (left) and vibration measurement location (right).

3.2.1 Results

3.2.1.1 Experiment 1

The vibrations were assessed at varying water pump frequencies. As already stated, each evaluation lasted 20 seconds. Figure 9 depicts the time-domain signals obtained from the accelerometer and LDV at a pump frequency of 50 Hz. Figure 10 illustrates the frequency domain of vibration responses from the accelerometer and LDV at a pump frequency of 50 Hz, as determined by the fast Fourier transform (FFT).

The accelerometer and LDV detected most of the frequency components, including the water pump frequency of 50 Hz and its harmonics at 100 Hz. A minor offset at around the 50 Hz frequency was noted, possibly the result of an uncalibrated frequency reading from the water pump. Interestingly, a prominent spike at 60 Hz was seen in the accelerometer data but not in the LDV data. This spike aligns with the electrical frequency, suggesting that the accelerometer may be affected by electromagnetic interference (EMI) to which the LDV is immune.

Figure 11 and Figure 12 show the FFTs of vibration responses at various pump frequencies for the accelerometer and LDV, respectively. Both devices detected all the water pump frequencies. However, a spike at 60 Hz was consistently seen in the accelerometer data, regardless of pump frequency. In the LDV data, this spike only appeared when the pump frequency was set at 60 Hz. This further confirms that EMI caused the accelerometer to always include the 60 Hz component.

Despite the EMI contamination at 60 Hz in the accelerometer signals, nearly all frequency features were captured and cross-verified by measurements from both devices.

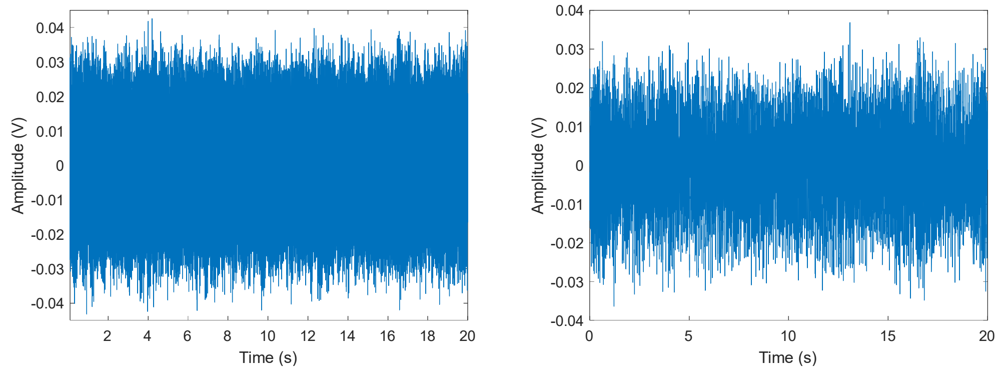

Figure 9. Time-domain signals at the water pump frequency of 50 Hz. (Left) Accelerometer. (Right) LDV.

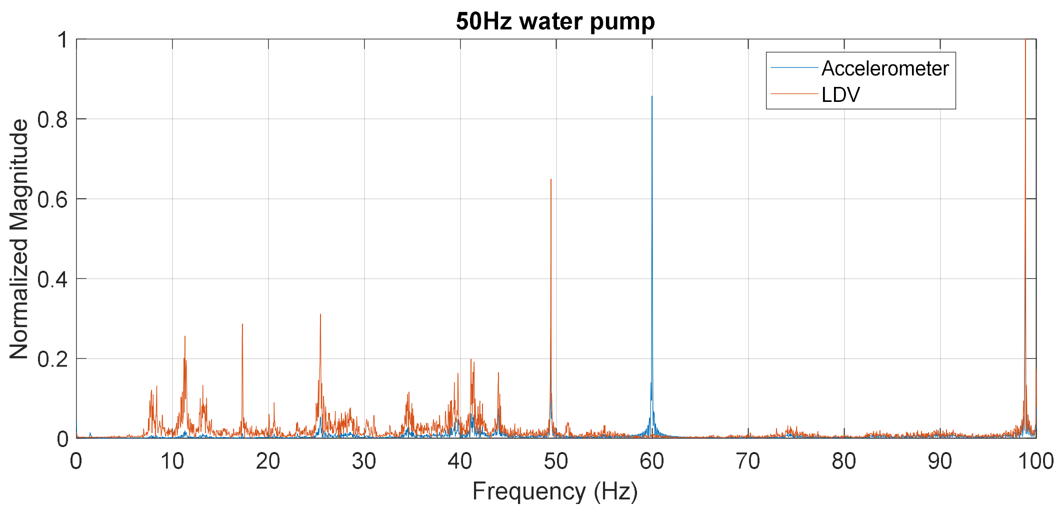

Figure 10. FFTs of vibration responses from the accelerometer and LDV at the pump frequency of 50 Hz.

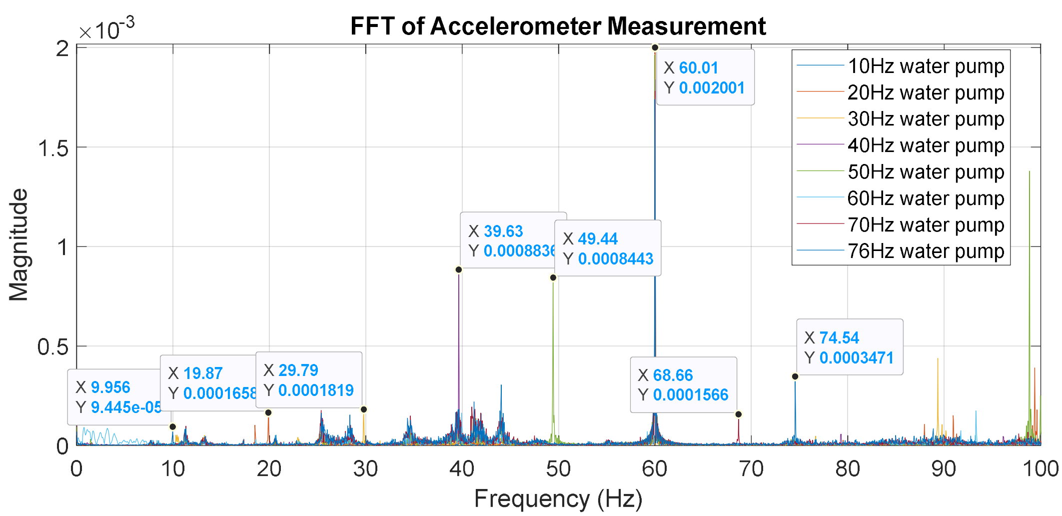

Figure 11. FFTs of vibration responses from the accelerometer at different pump frequencies.

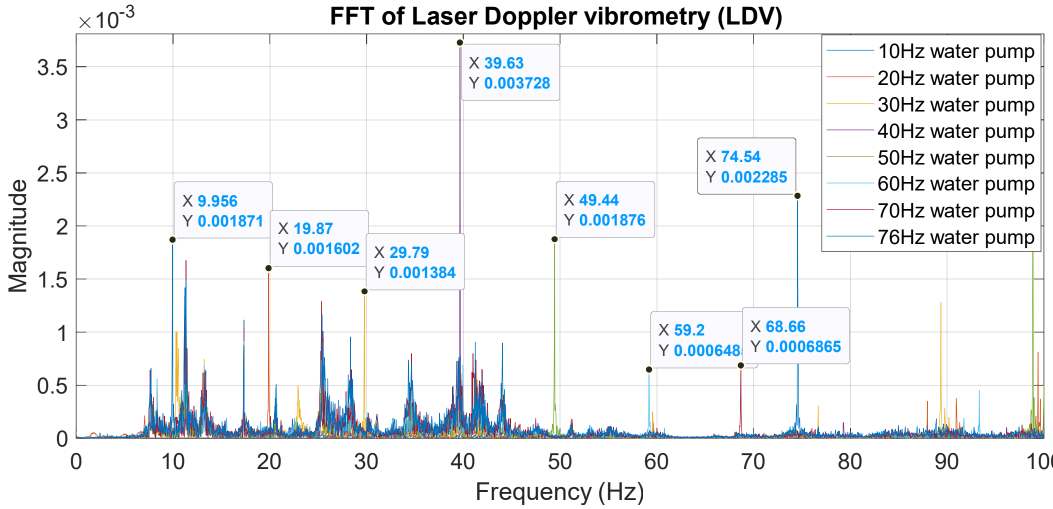

Figure 12. FFTs of vibration responses from the LDV at different pump frequencies.

3.2.1.2 Experiment 2

In the second experiment, vibration was continuously measured while manually adjusting the water pump frequency from 65 to 75 Hz, then decreasing it to 5 Hz in increments of 5 Hz. Following these adjustments, the pump was finally turned off. The entire experiment lasted 500 seconds. Figure 13 and Figure 14 display the time-domain signals captured by the accelerometer and LDV, respectively. Noticeably, the vibration amplitudes at 65 Hz are significantly higher than those at other pump frequencies, likely because 65 Hz is near one of the natural frequencies of the FAS.

To analyze frequency over time, we used the short-time Fourier transform. Figure 15 and Figure 16 show the spectrograms of the waveforms given in Figure 13 and Figure 14, respectively, with only the frequencies below 100 Hz displayed. In the figures, the varying water pump frequencies are clearly visible. As anticipated, a dominant 60 Hz frequency persists throughout the entire duration, due to EMI-something not observed in the LDV measurement.

Figure 17 and Figure 18 present spectrograms ranging from 0 to 500 Hz. These clearly show the harmonics of the water pump frequencies—harmonics that are 6 times greater than those the water pump frequencies. In Figure 17, a 360 Hz frequency (6 × 60 Hz) is absent throughout the measurement duration, confirming that the 60 Hz frequency stems from EMI and only served to affect the data acquisition system. Comparison of the harmonics (see Figure 17 and Figure 18) reveals that both the accelerometer and LDV captured identical frequency components, including data obtained when transitioning from one pump frequency to another. For instance, both devices captured a dip that occurred at around the 230-second mark.

3.2.1.3 Summary

In this experiment, both the accelerometer and LDV effectively captured the vibration responses on the main pipe of the FAS. The data acquisition system for the accelerometer was influenced by EMI at the 60 Hz frequency, an issue that warrants further investigation. In contrast, the LDV system proved immune to EMI.

Despite this, the accelerometer does offer certain advantages over the LDV system, such as being less expensive and easier to set up. The LDV system, while more expensive, offers cleaner vibration measurements. It also boasts a broad measurement range (from DC to 24 MHz), making it suitable for most practical applications. Furthermore, the LDV's capability for remote measurement makes it a viable option for harsh environments such as ones involving high temperatures or radiation levels.

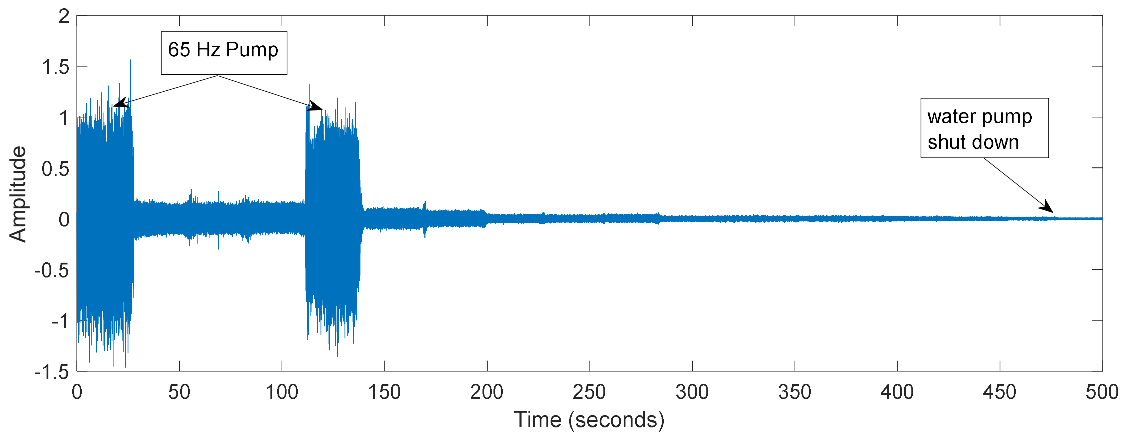

Figure 13. Time-domain signal received by the accelerometer.

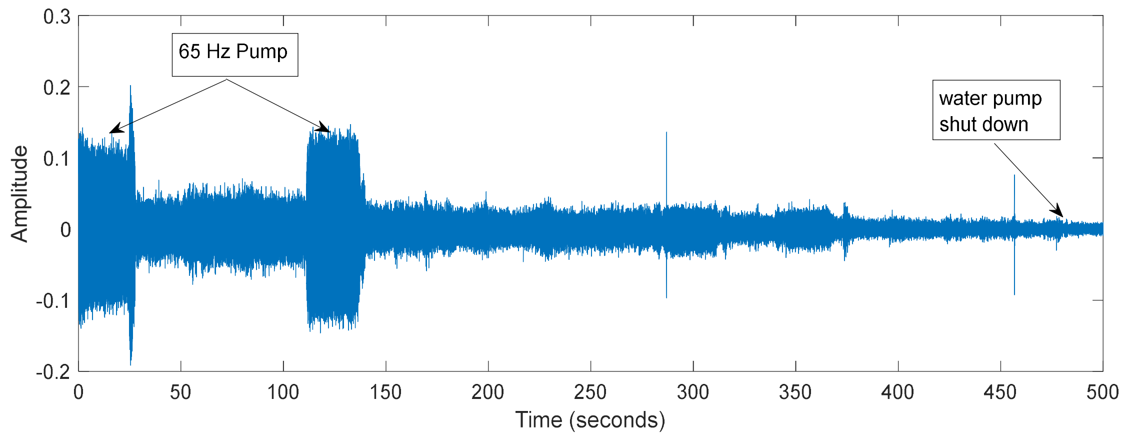

Figure 14. Time-domain signal received by the LDV.

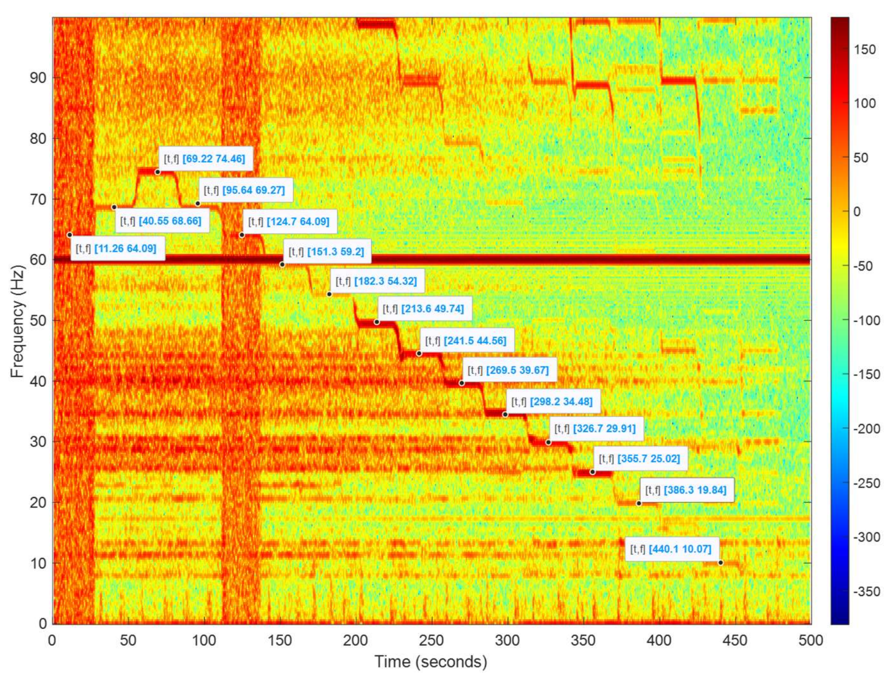

Figure 15. Spectrogram of the waveform captured by the accelerometer at 0–100 Hz.

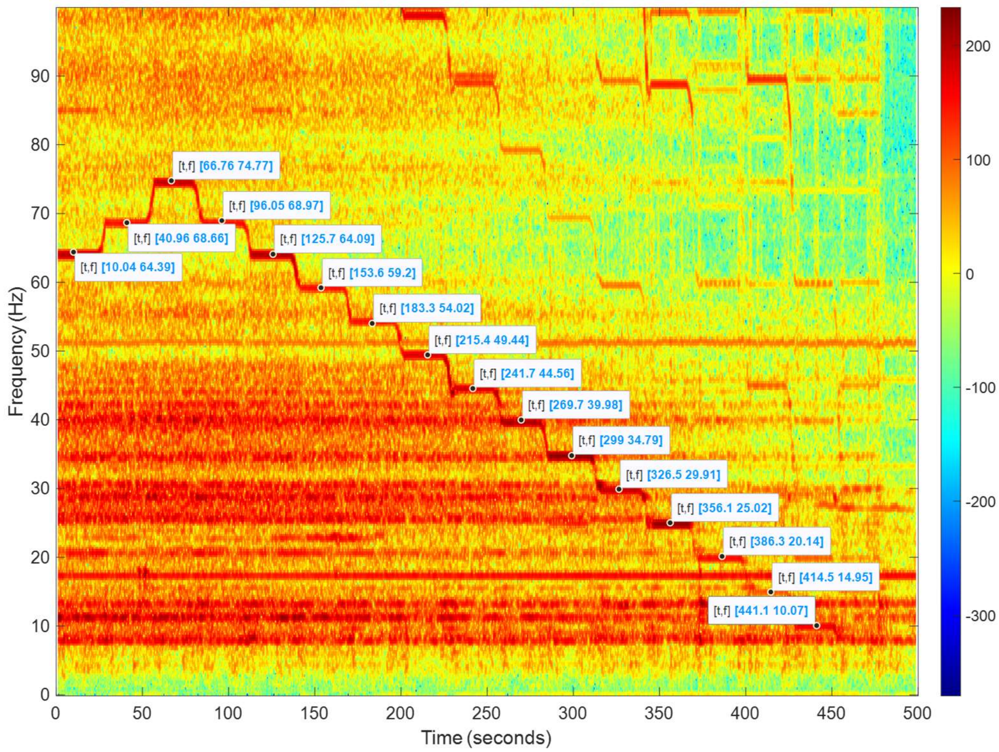

Figure 16. Spectrogram of the waveform captured by the LDV at 0-100 Hz.

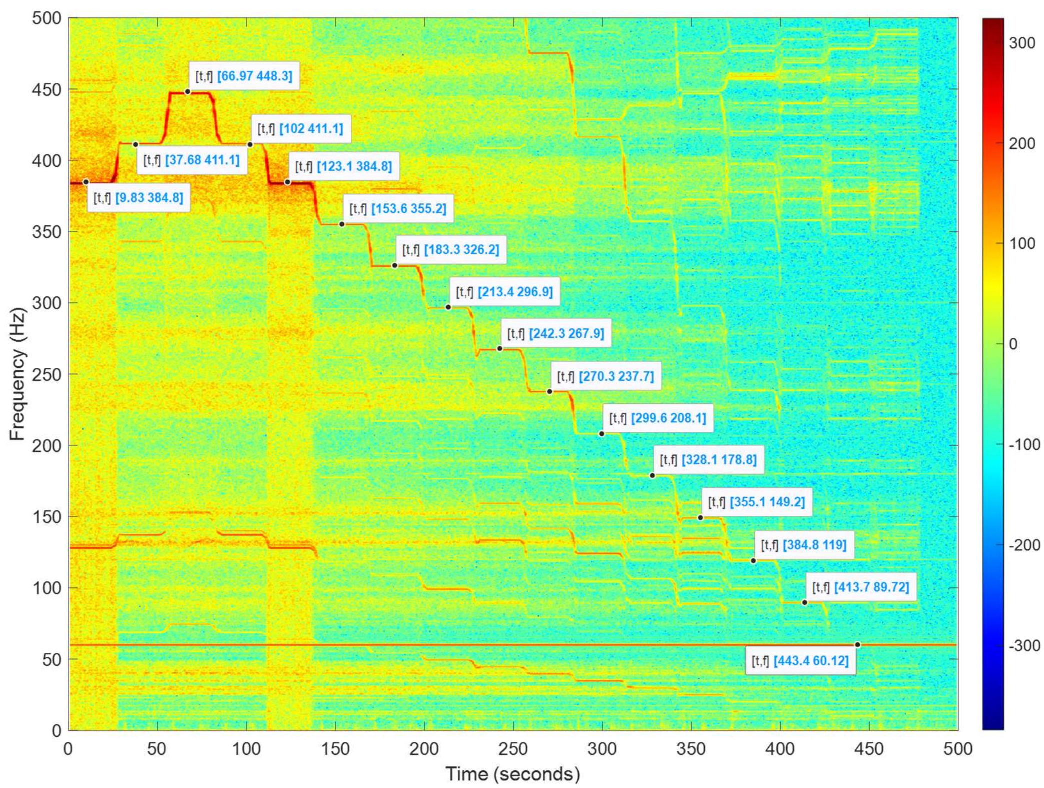

Figure 17. Spectrogram of the waveform captured by the accelerometer at 0–500 Hz.

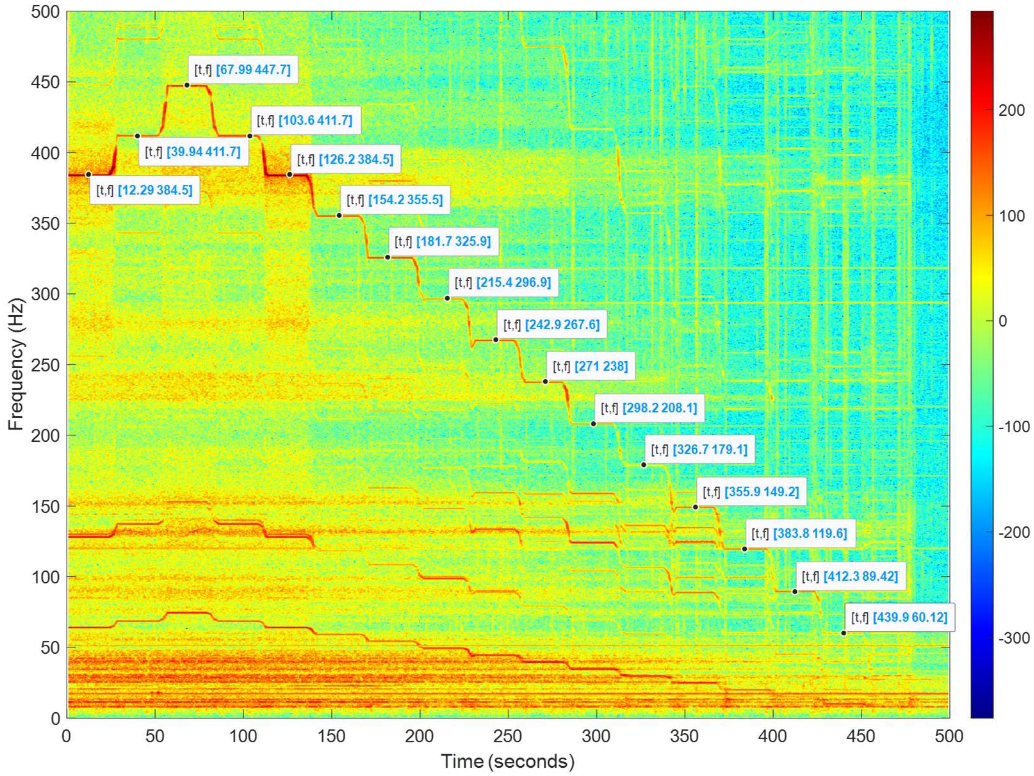

Figure 18. Spectrogram of the waveform captured by the LDV at 0–500 Hz.

4. DEVELOPMENT PLAN

Although the commercially available sensors/transducers may be useful for ex-vessel monitoring of components within a light-water reactor power plant, the small size and higher operating temperatures of developmental advanced reactors necessitate transducers with higher temperature and radiation tolerances. For in-core applications (i.e., test reactors), these conditions are even more severe. Thus, significant challenges must be overcome for the development of improved sensors/transducers. Among these identified challenges are:

- Material selection
  - High-temperature and radiation-tolerant active materials
  - Electrode or coil materials and dielectrics
  - Housing fill and acoustic damping materials
  - Housing materials compatible with likely environments (i.e., corrosive coolants)
- Design considerations
  - Bonding of active material to protective wear face
    - Thermal expansion mismatches and chemical compatibility are key
  - Coupling of AE sensors to structures
  - Seismic mass for vibration sensors
  - Damping to reduce ringing

- Steps for development
  - Technology selection:
    - Investigate various acoustic sensor technologies (e.g., piezoelectric, magnetostrictive, and micromachined mlectro-mechanical sensors), and select the most suitable for specific application requirements
    - Consider factors such as sensitivity, bandwidth, and robustness against environmental factors
  - Material selection:
    - Choose appropriate materials for the sensor's active element, with radiation tolerance being a key factor
    - Choose structural materials that are compatible with the chemical environment
    - Materials used in construction must also be compatible with each other
  - Design and prototyping:
    - Develop a detailed design for the AE sensor, including the transducer, signal conditioning circuitry, and data acquisition system
    - Utilize simulation tools to model the sensor's behavior under different conditions
    - Create prototypes for testing and validating the design's functionality and sensitivity
  - Fabrication and manufacturing:
    - Establish a repeatable fabrication process
    - Implement quality control measures to maintain consistent sensor performance
  - Testing and calibration:
    - Conduct extensive testing to evaluate the sensor's sensitivity, frequency response, and noise tolerance
    - Calibrate the sensor to ensure accurate AE detection and measurement
    - Perform tests at high temperatures
    - Perform irradiation testing in gamma and mixed gamma-neutron environments
  - Iterative optimization:
    - Analyze the test results to identify necessary design improvements.

5. REFERENCES

1. Daw, J., et al. 2023. “Assessment of Acoustic Sensor Application to Structural Health Monitoring of Reactor Components.” Idaho National Laboratory. INL/RPT-23-70721.

2. Favretto-Cristini, N., Hégron, L., and Sornay, P. 2016. “Identification of the fragmentation of brittle particles during compaction process by the acoustic emission technique.” *Ultrasonics*. **67**, 178-189, ISSN 0041-624X. https://doi.org/10.1016/j.ultras.2015.12.010.

3. Marklund, A. R. and Dufek, J. 2014. “Development and comparison of spectral methods for passive acoustic anomaly detection in nuclear power plants.” *Applied Acoustics*. **83**, 100-107, ISSN 0003-682X. https://doi.org/10.1016/j.apacoust.2014.03.014.

4. Hill, J. W. 2018. “Acoustic Emission Detection In 304H Stainless Steel Due To Intergranular Stress Corrosion Cracking.” University of South Carolina: University Libraries, Master's thesis. https://scholarcommons.sc.edu/etd/4902.

5. Pauw, B.D., et al. 2017. “Characterizing Flow-Induced Vibrations of Fuel Assemblies for Future Liquid Metal Cooled Nuclear Reactors Using Quasi-Distributed Fibre-Optic Sensors.” *Appl. Sci.* **7**, (8): 864. https://doi.org/10.3390/app7080864.

6. Romrell, D. M. 1972. “Acoustic emission weld monitoring of nuclear components.” United States. https://doi.org/10.2172/5061062.

7. Ko, D-Y. and Kim, K-H. 2013. “Design of a vibration and stress measurement system for an advanced power reactor 1400 reactor vessel internals comprehensive vibration assessment program,” *Nuclear Engineering and Technology*. **45**, (2): 249-256, ISSN 1738-5733. https://doi.org/10.5516/NET.09.2012.049.

8. Damiano, B. and Kryter, R. C. 1990. “Current Applications of Vibration Monitoring and Neutron Noise Analysis: Detection and Analysis of Structural Degradation of Reactor Vessel Internals from Operational Aging.” NUREG/CR-5479, ORNL/TM-11398, Oak Ridge National Laboratory, Oak Ridge, Tenn. https://www.nrc.gov/docs/ML0403/ML040350086.pdf.

9. Reinhardt, B., Daw, J., and Tittmann, B. R. 2018. “Irradiation Testing of Piezoelectric (Aluminum Nitride, Zinc Oxide, and Bismuth Titanate) and Magnetostrictive Sensors (Remendur and Galfenol).” IEEE Transactions on Nuclear Science. **65**, (1): 533-538. https://doi.org/10.1109/TNS.2017.2775163.

10. Chen, L., et al. 2023. “Scandium-Doped Aluminum Nitride for Acoustic Wave Resonators, Filters, and Ferroelectric Memory Applications.” *ACS Applied Electronic Materials*. **5**, (2): 612-622. https://doi.org/10.1021/acsaelm.2c01409.

11. Calderoni, P. 2020. “Advanced Sensors and Instrumentation.” Idaho National Laboratory. (12). https://www.energy.gov/sites/prod/files/2020/05/f74/ne-asi-newsletter-issue-12-032020.pdf.